Supporting Information

Facile Design and Fabrication of Superwetting Surfaces with Excellent Wear-Resistance

Wenbo Zhang,[†] *Tianhao Xiang,*[†] *Feng Liu,*[†] *Ming Zhang,* [†, ‡] *Wentao Gan,*[†] *Xianglin Zhai,*[§] *Xin Di,*[†] *Yazhou Wang,*[†] *Guoxiang Liu*[†] *and Chengyu Wang**[, †]

[†]Key Laboratory of Bio-Based Material Science and Technology of Ministry of Education, Northeast Forestry University, Harbin, 150040, P. R. China

[‡]Department of Materials Science and Engineering, University of Pennsylvania, 216 LRSM Building, 3231 Walnut Street, Philadelphia, PA 19104, USA

[§]Department of Chemistry, Louisiana State University, Baton Rouge, LA 70803, USA

*To whom all correspondence should be addressed

Email: wangcy@nefu.edu.cn

Tel (Fax): +86-451-82190116

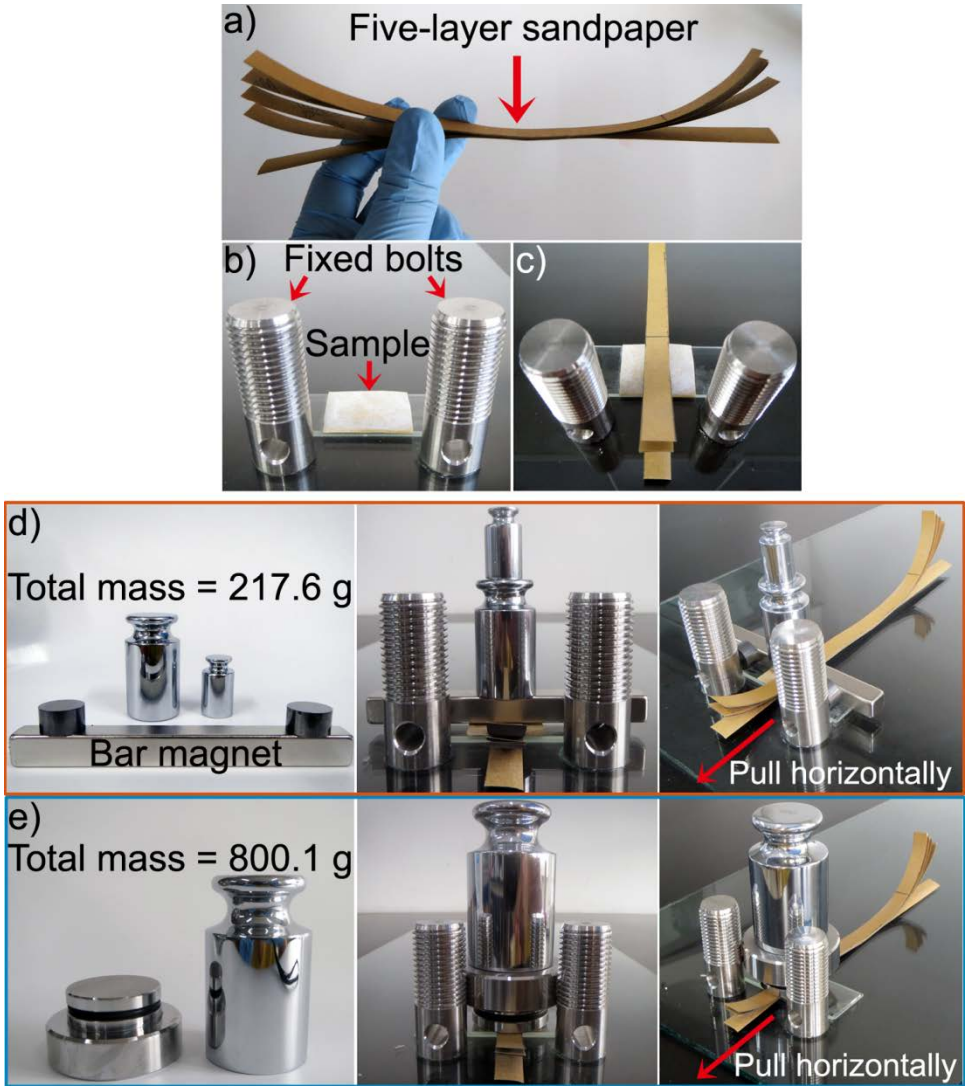

Figure S1. The apparatus used for abrasion tests.

Abrasion tests: Five pieces of sandpaper (grit no. 600 or 320) with a same width of 1 cm were stuck together (Figure S1a) as the abradant. The sample was immobilized through two fixed stainless-steel bolts (Figure S1b) and the rough texture of the abradant was in direct contact with the sample (Figure S1c). For the moderate wear, grit no. 600 sandpaper, the abraded area of 1 cm × 0.9 cm and a pressure of 24 kPa were adopted, as shown in Figure S1d; for the severe abrasion, grit no. 320 sandpaper, the abraded area of 1 cm × 2.5 cm and a pressure of 32 kPa were adopted, as shown in Figure S1e. We pulled the sandpaper horizontally and linearly on the sample and the distance traveled by the sandpaper in each cycle is 10 cm.

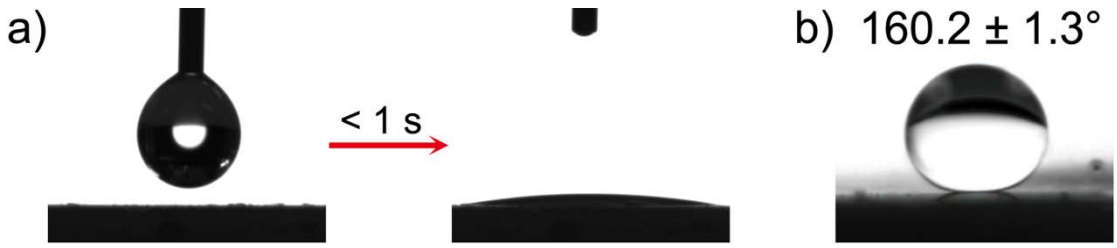

Figure S2. a) Wettability of the superhydrophilic surface toward water (5 μL) in air. (b) Wettability of the superhydrophilic surface toward oil (1, 2-dichloroethane, 5 μL) underwater.

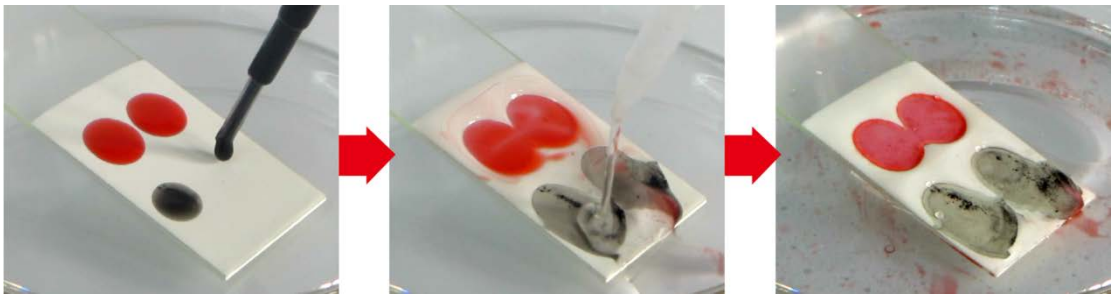

Figure S3. Contamination of a superhydrophilic surface by the tinted corn oils (tinted by Sudan III and Fe_3O_4).

The unwetted superhydrophilic nylon/SiO_2 coating can be easily contaminated by the tinted corn oils. Consequently, the oils formed stable oil-barrier layers to eliminate pinning of water.

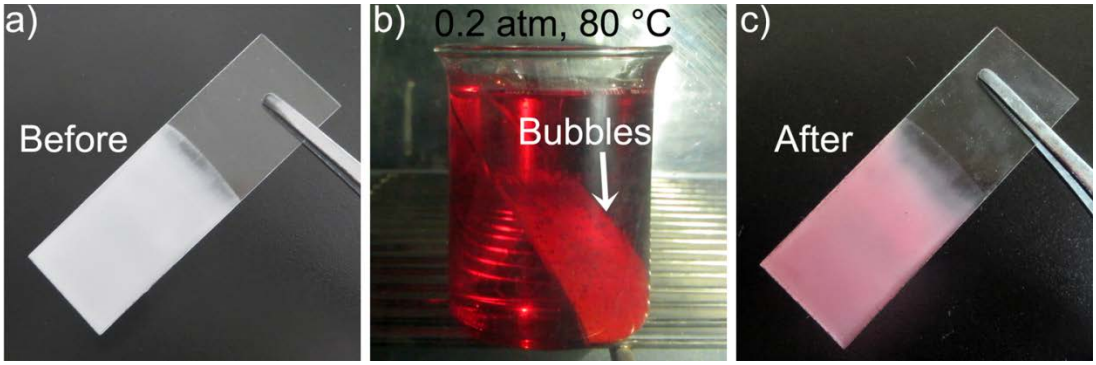

Figure S4. Contamination of a WBORS in a high-temperature/low-pressure oily environment (red: tinted corn oil). The water-barrier layer on the WBORS disappeared entirely after the high-temperature/low-pressure process, leaving a contaminated surface.

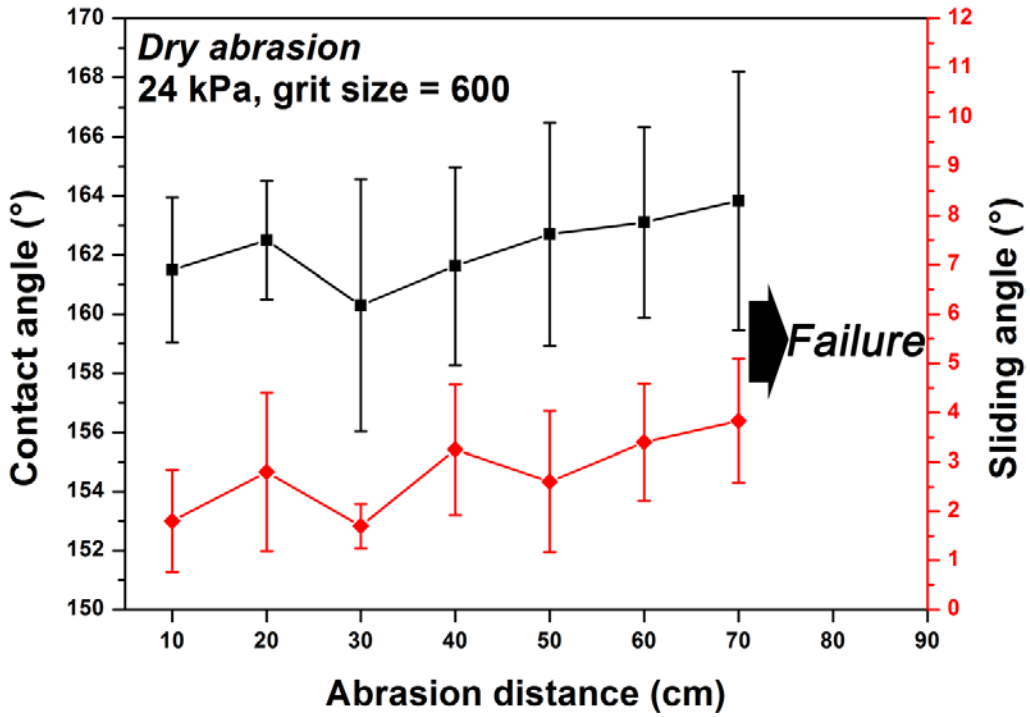

Figure S5. Variation of underwater OCA and OSA of the unwetted resin-immobilized coating with increasing abrasion distances of grit no. 600 sandpaper under a pressure of 24 kPa.

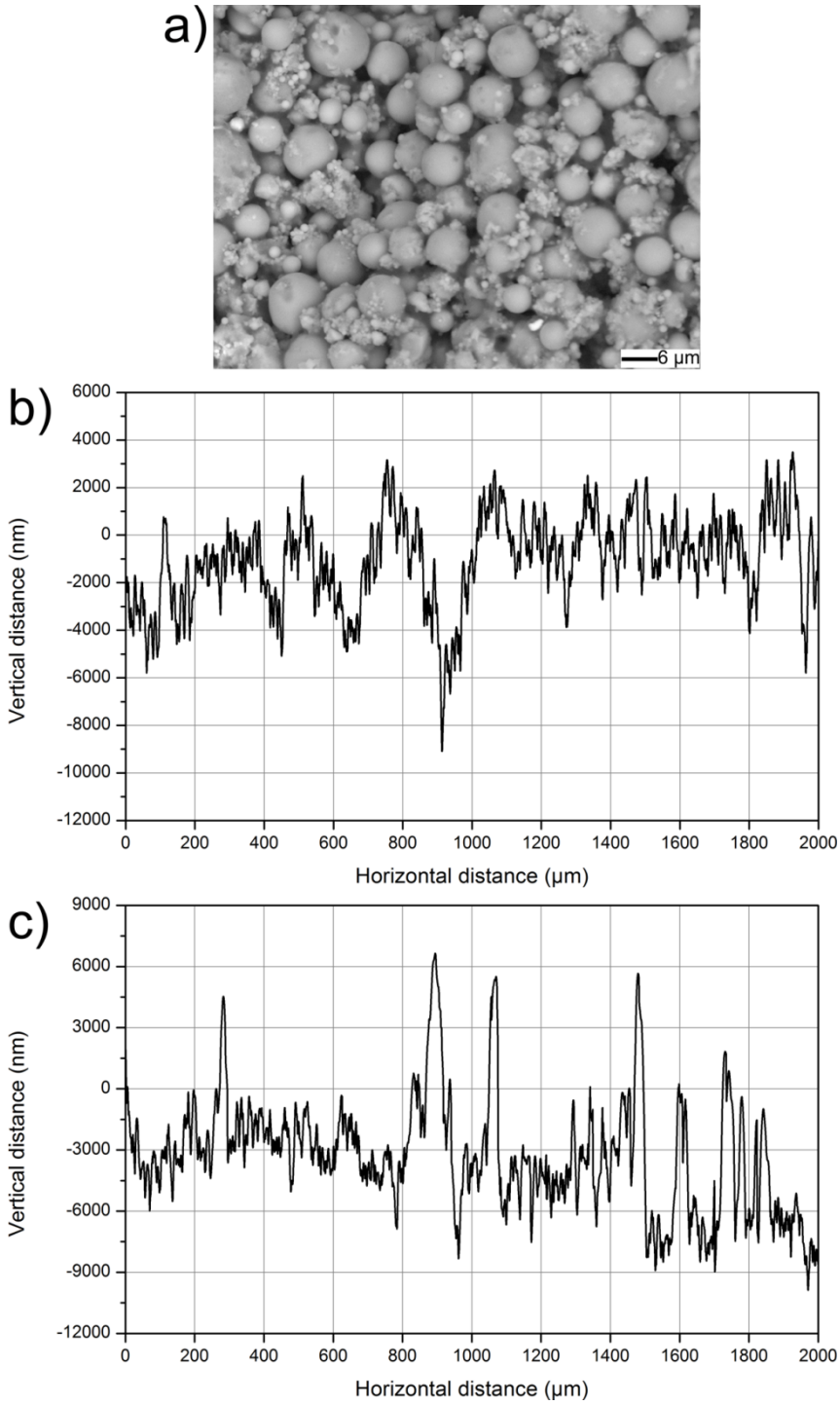

Figure S6. a) SEM image of the unwetted resin-immobilized coating after the 10 cm abrasion with grit no. 600 sandpaper under a pressure of 24 kPa. Surface height profiles of the resin-immobilized coating before (a) and after (b) the 10 cm abrasion.

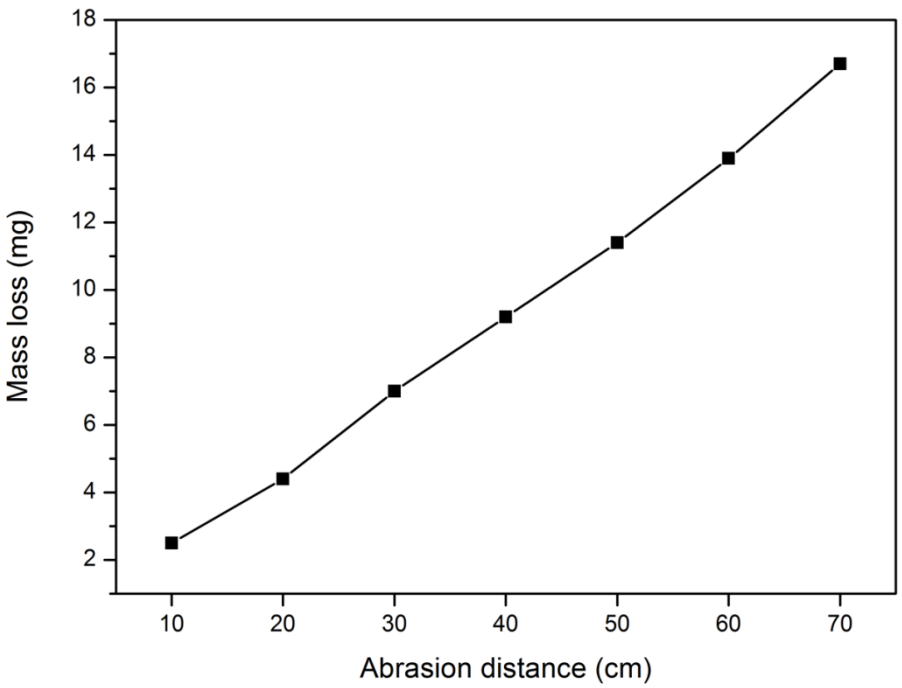

Figure S7. Variation of total mass loss of the unwetted resin-immobilized coating with increasing abrasion distances of grit no. 600 sandpaper under a pressure of 24 kPa.

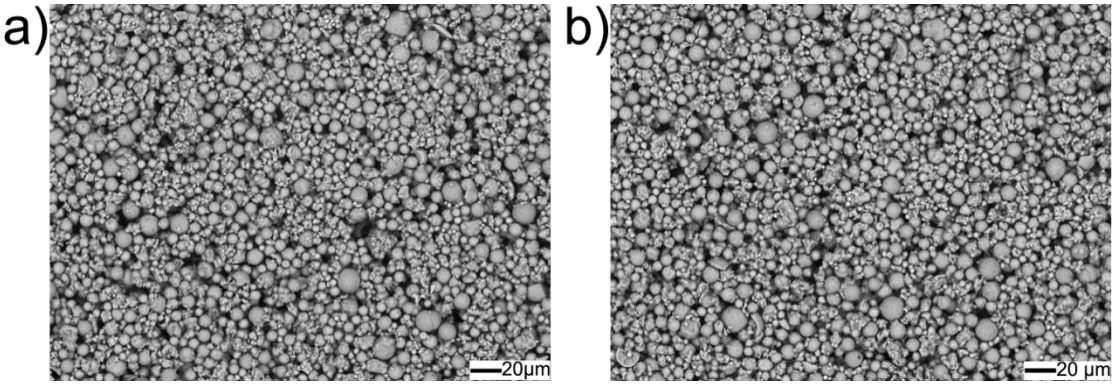

Figure S8. SEM images of the resin-immobilized coating before (a) and after (b) the vertical water jet scouring test.

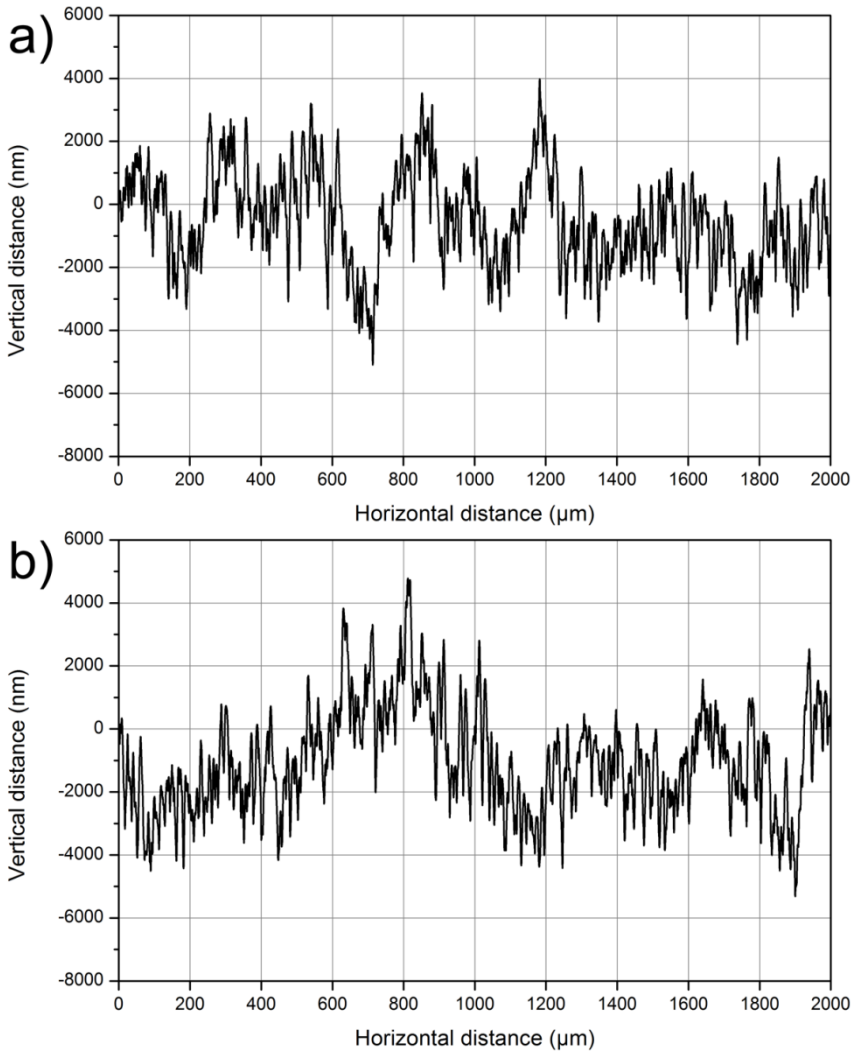

Figure S9. Surface height profiles of the resin-immobilized coating before (a) and after (b) the vertical water jet scouring test.

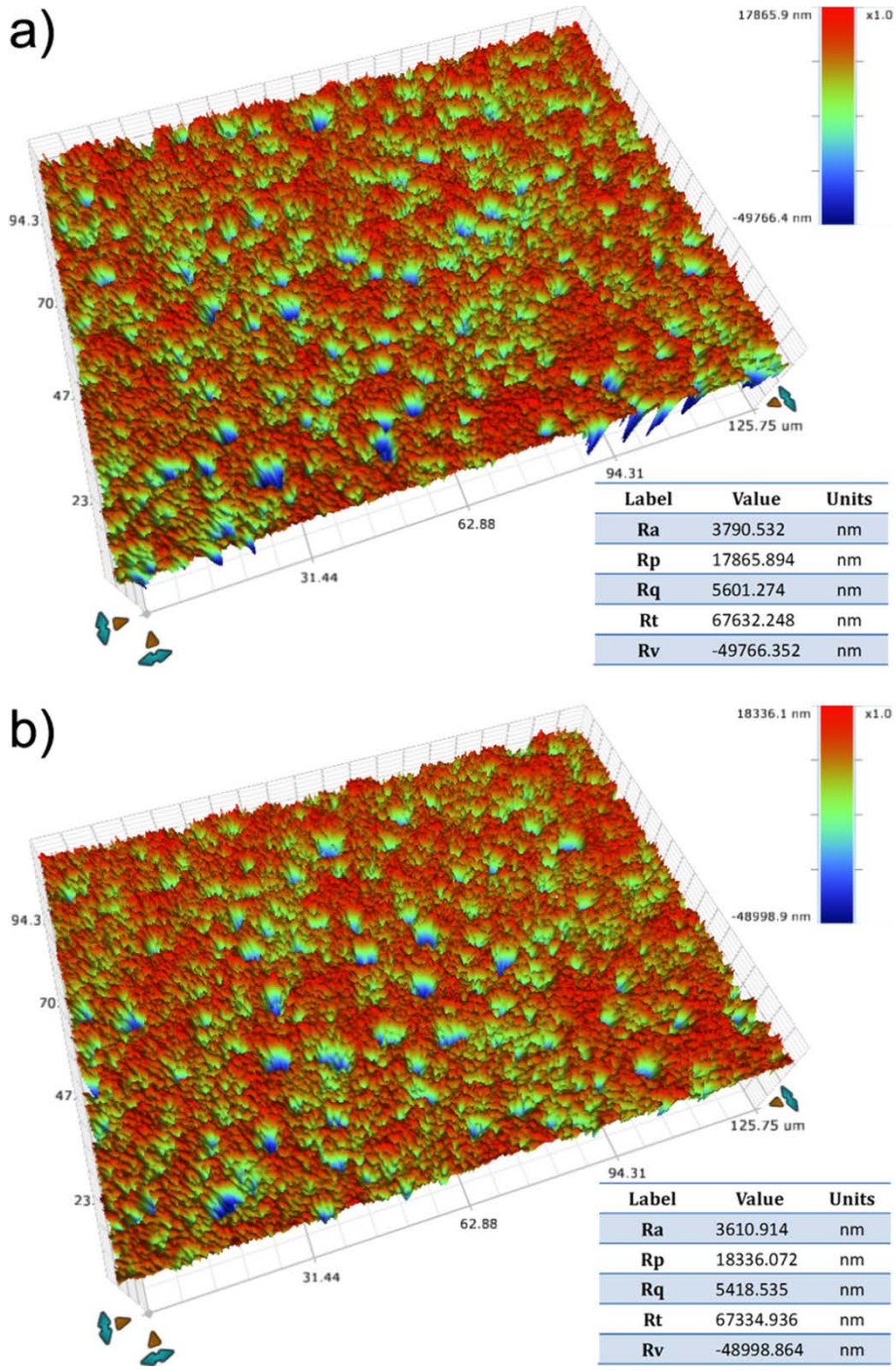

Label	Value	Units
Ra	3790.532	nm
Rp	17865.894	nm
Rq	5601.274	nm
Rt	67632.248	nm
Rv	-49766.352	nm

Label	Value	Units
Ra	3610.914	nm
Rp	18336.072	nm
Rq	5418.535	nm
Rt	67334.936	nm
Rv	-48998.864	nm

Figure S10. 3-D roughness profiles of the resin-immobilized coating before (a) and after (b) the vertical water jet scouring test (Ra, arithmetical mean deviation of the profile; Rp, maximum height of the profile; Rq, root-mean-square deviation of the profile; Rt, total height of the profile; Rv, maximum depth of the profile).

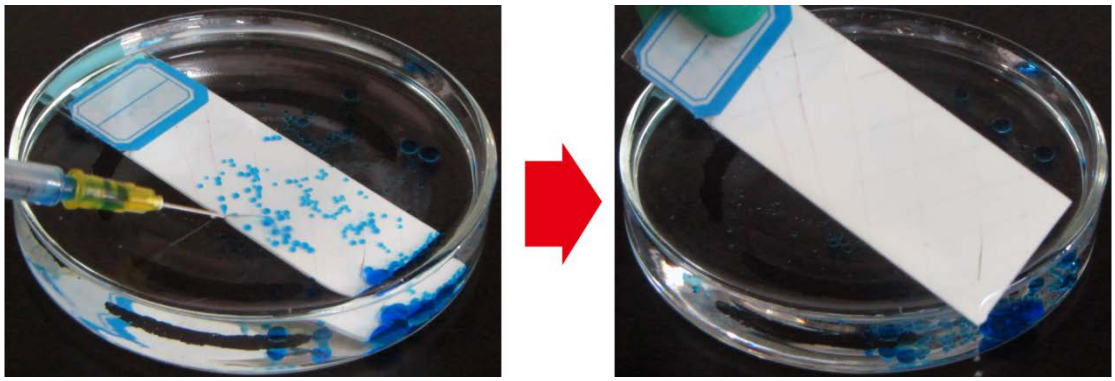

Figure S11. Ability to repel tiny oil droplets (carbon tetrachloride, tinted by Sudan Blue II) underwater by the knife-scratched WBORS.

The oil extruded from a syringe needle (25 G) dropped on the knife-scratched WBORS underwater and readily rolled off it, indicating retained oil repellency.

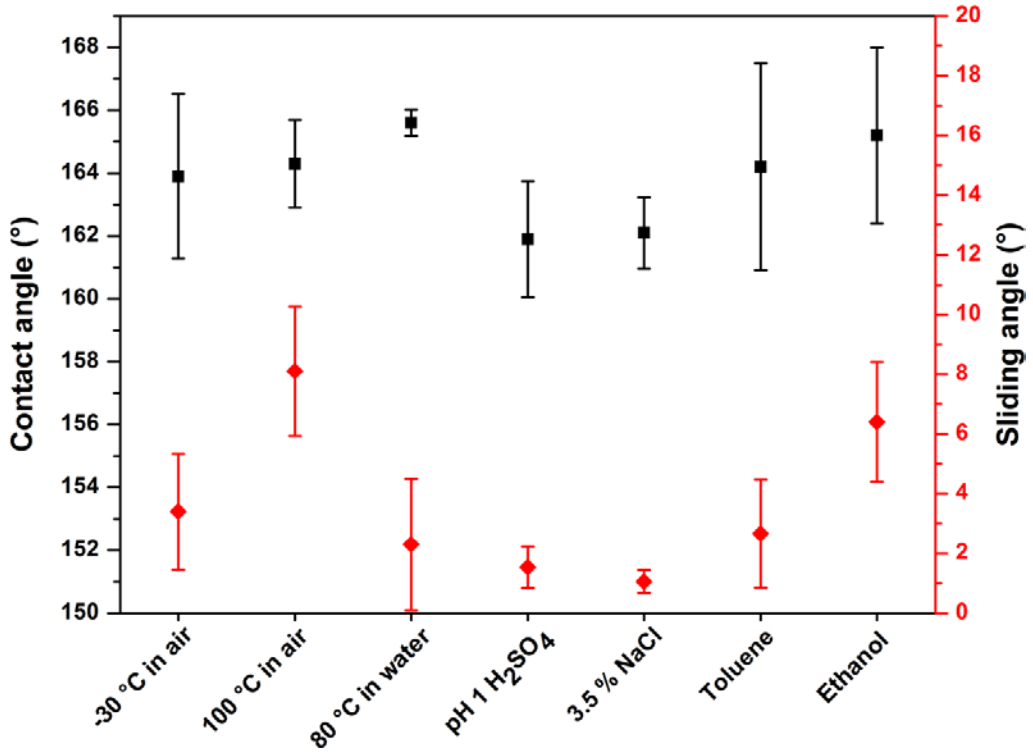

Figure S12. The underwater OCAs and OSAs of the resin-immobilized coatings after the tests in various circumstances.

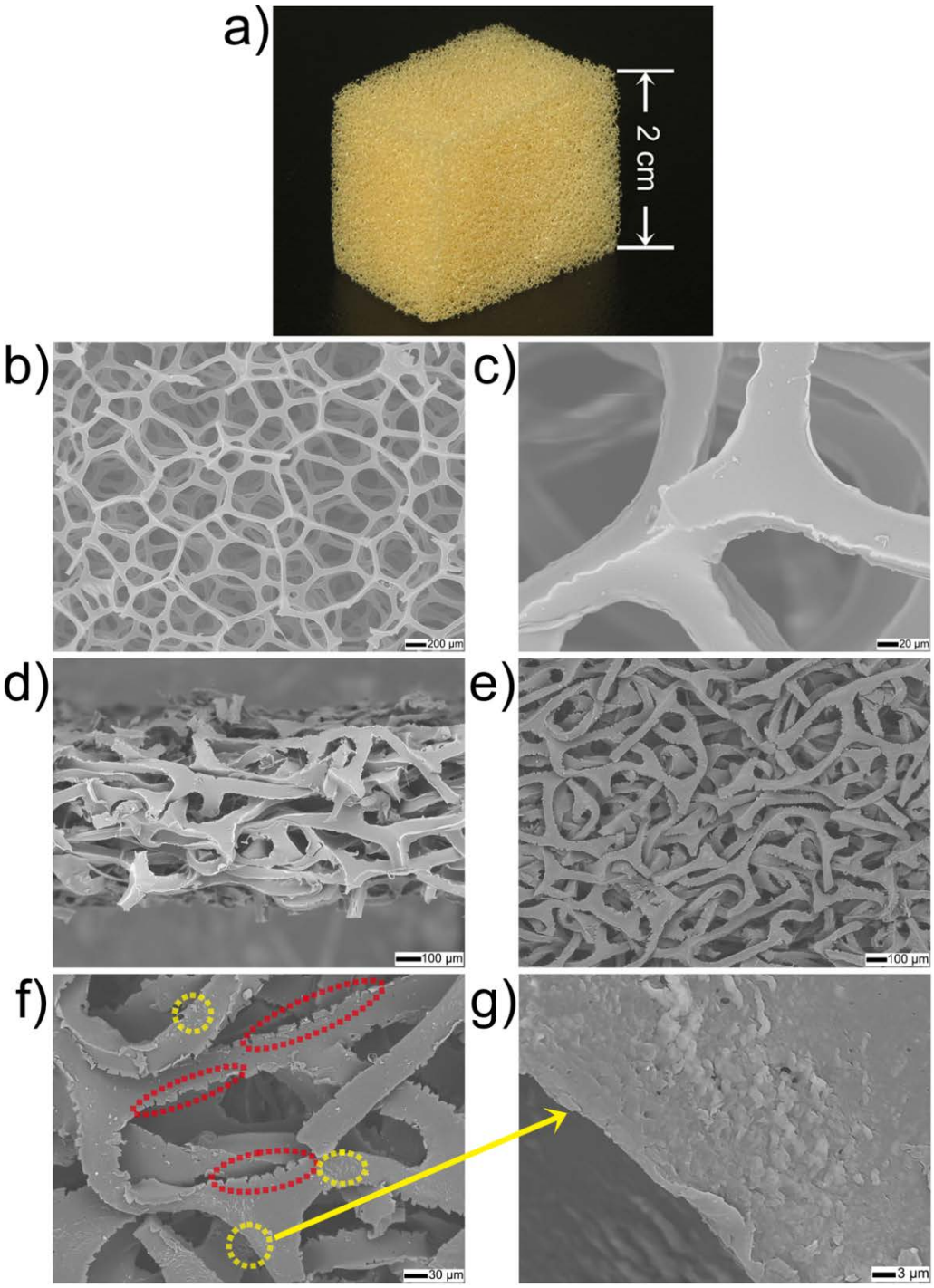

Figure S13. a) Photograph of raw PU foam with a height of 2 cm. SEM images for (b, c) raw PU foam; d) cross section of an unfilled cushion; e, f) the top surface of the unfilled cushion. The jagged cracks and the submicrometer-sized protrusions in (f) are highlighted in red and yellow, respectively; g) high-magnification morphology of the submicrometer-sized protrusions.

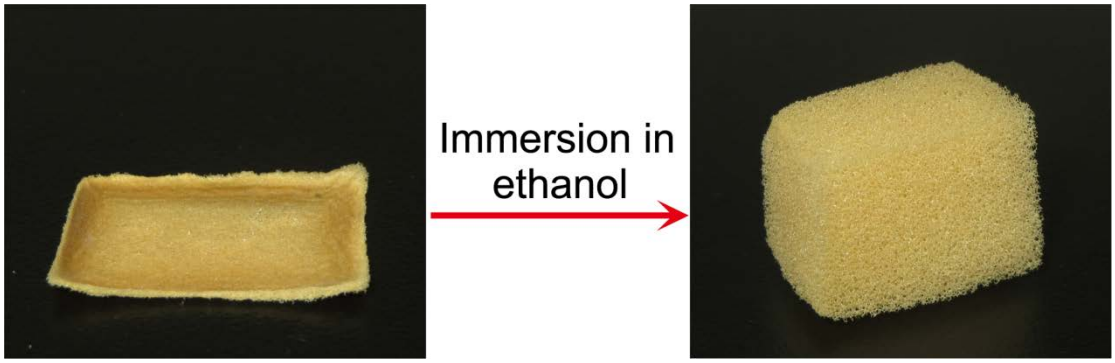

Figure S14. The appearance restoration of compacted PU foam (without adhesive processing) in ethanol.

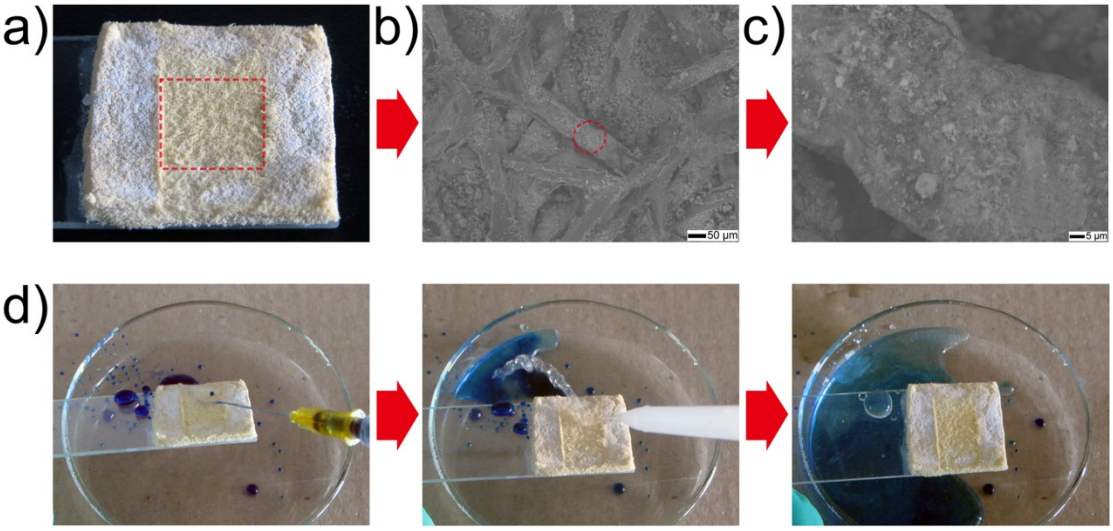

Figure S15. a) Photograph of the NFCPC after the 1000 cm abrasion with grit no. 600 sandpaper under a pressure of 24 kPa. Abraded area (1 cm × 0.9 cm) is highlighted in red. b, c) Corresponding SEM images for the top surface of the worn NFCPC. d) Water repellency for tiny and large droplets of the NFCPC worn to 1000 cm, indicating durable non-wettability.

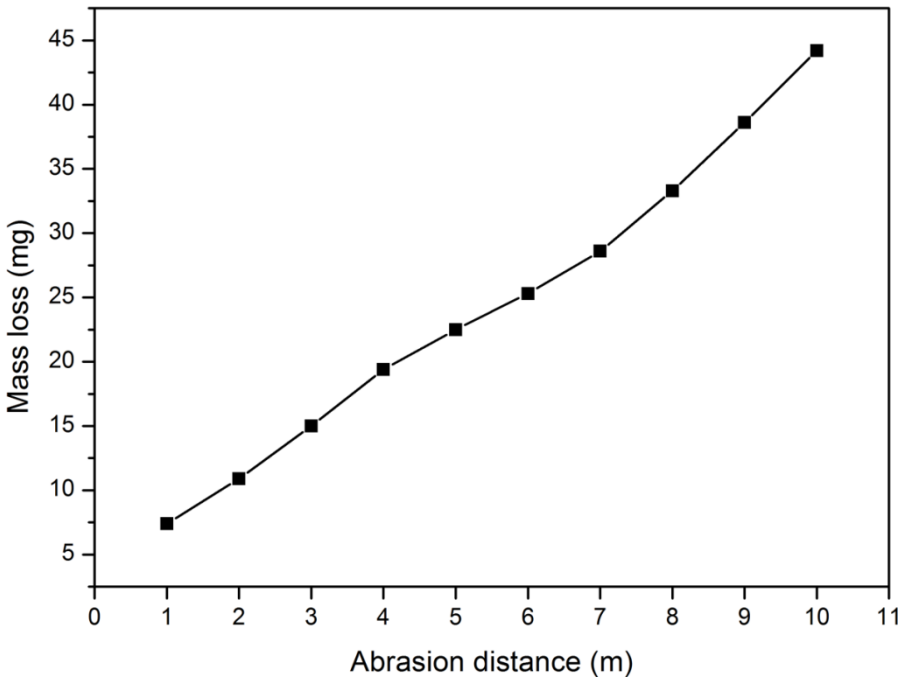

Figure S16. Variation of total mass loss of the NFCPC with increasing abrasion distances of grit no. 600 sandpaper under a pressure of 24 kPa.

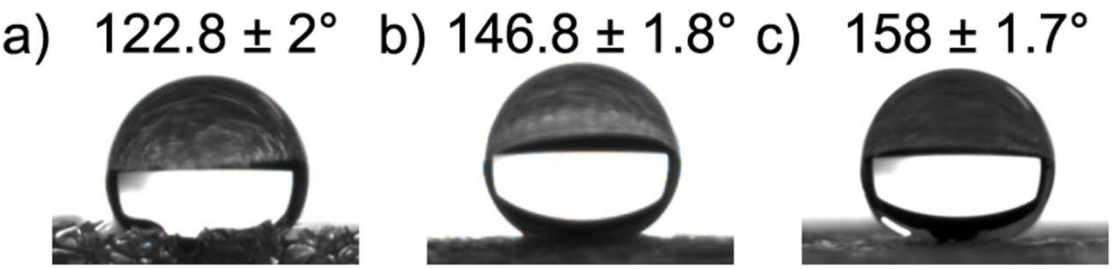

Figure S17. Water contact angle images of (a) raw PU foam, (b) an unfilled cushion and (c) an NFCPC.

For the pristine foam (Figure S17a), the water contact angle is 122.8 ± 2°, exhibiting its intrinsic hydrophobicity; the physical compression and the fluoridation resulted in increased water repellency of PU, and quasi-superhydrophobicity was obtained (Figure S17b); the introduction of nanoroughness conduced to a higher water contact angle (Figure S17c) and complete non-wettability.

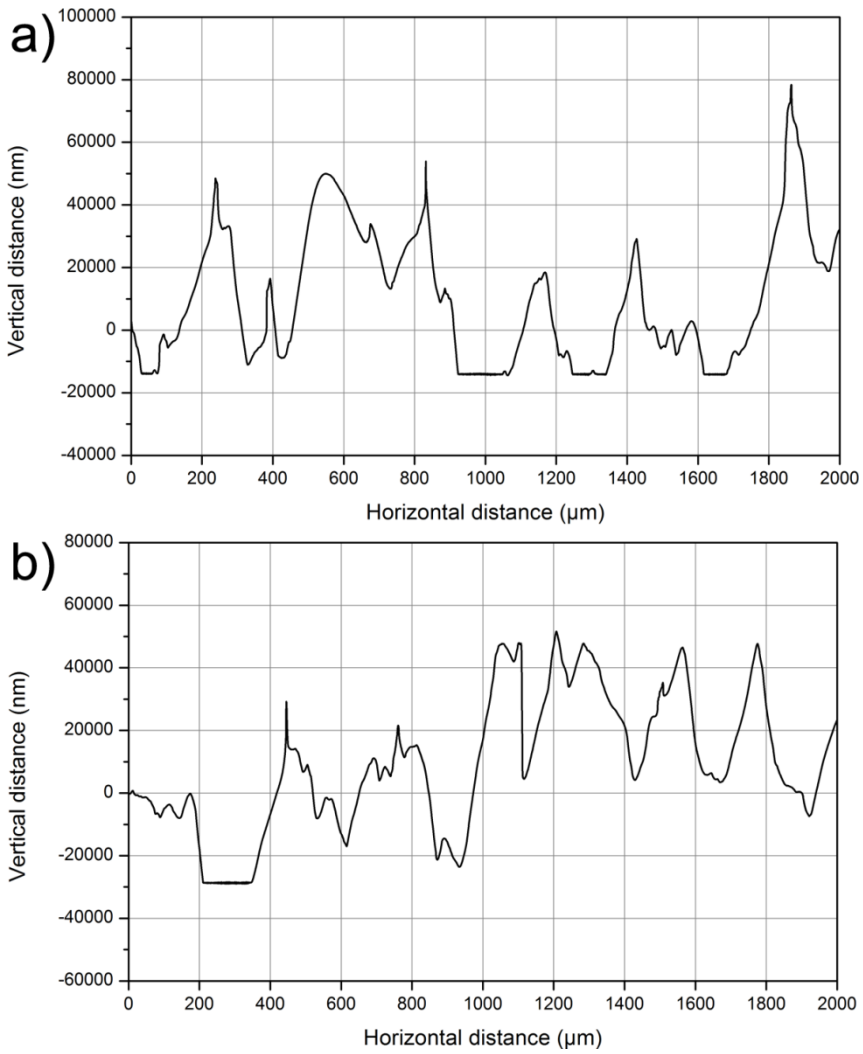

Figure S18. Surface height profiles of the NFCPC before (a) and after (b) the 100 cm abrasion with grit no. 600 sandpaper under a pressure of 24 kPa.

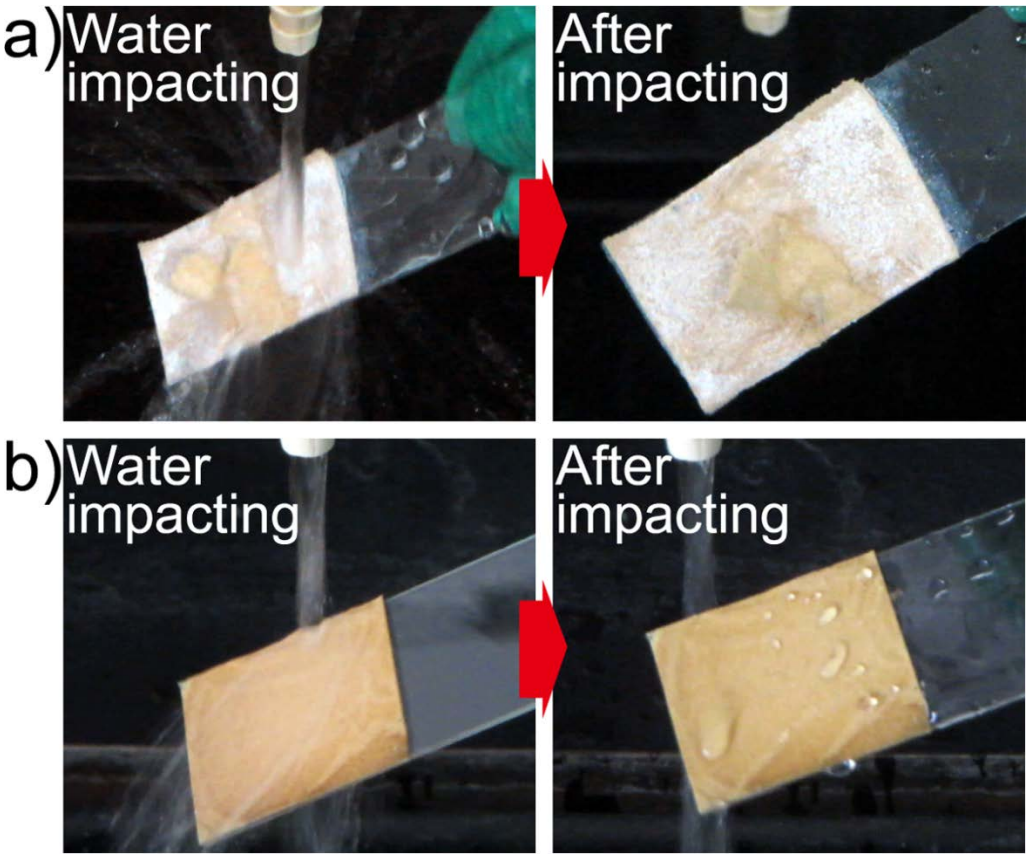

Figure S19. Water impact tests on (a) the severely worn NFCPC and (b) an unfilled cushion.

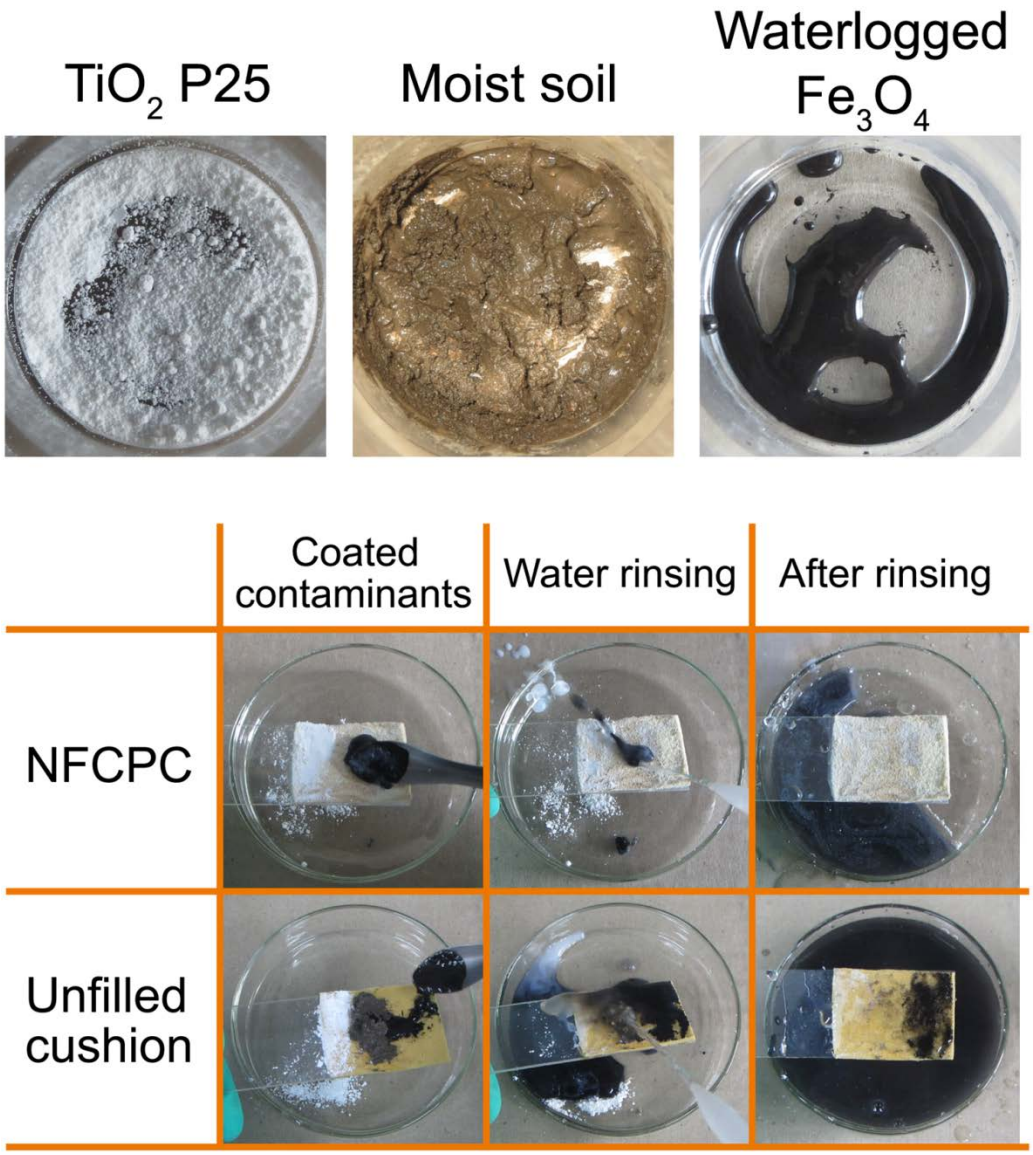

Figure S20. Self-cleaning tests on an NFCPC and an unfilled cushion.

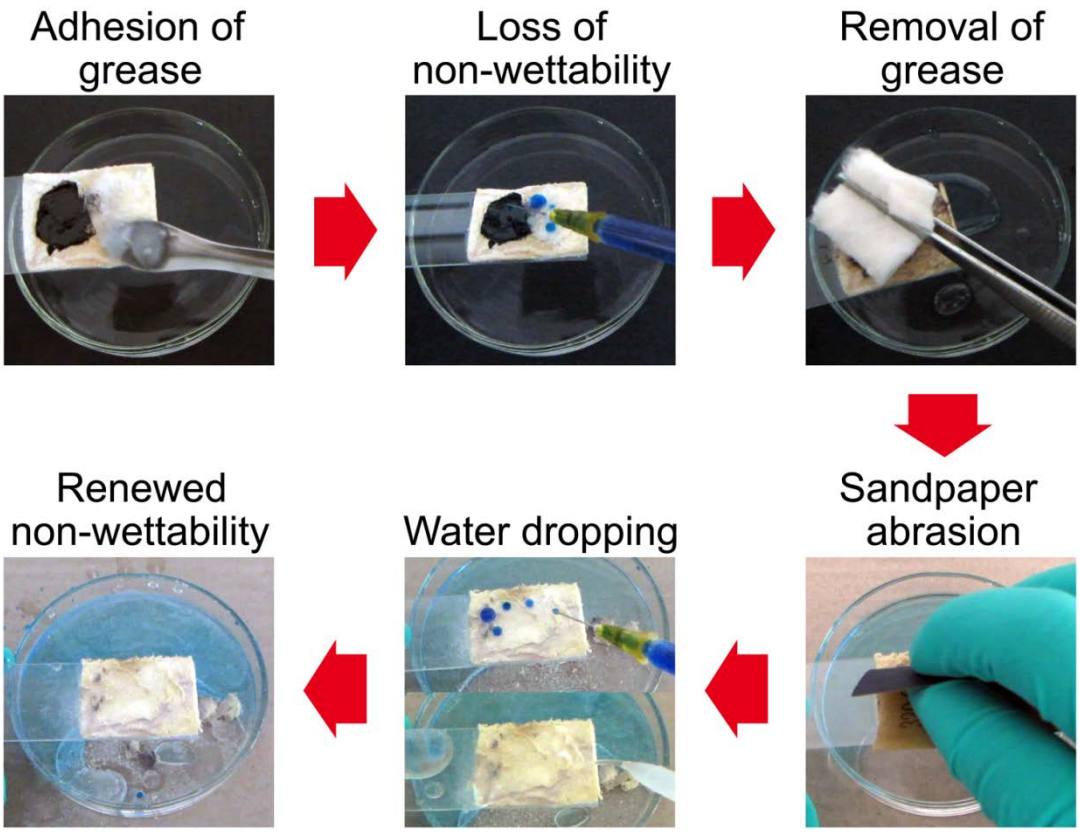

Figure S21. Regeneration of non-wettability for a grease-contaminated NFCPC.

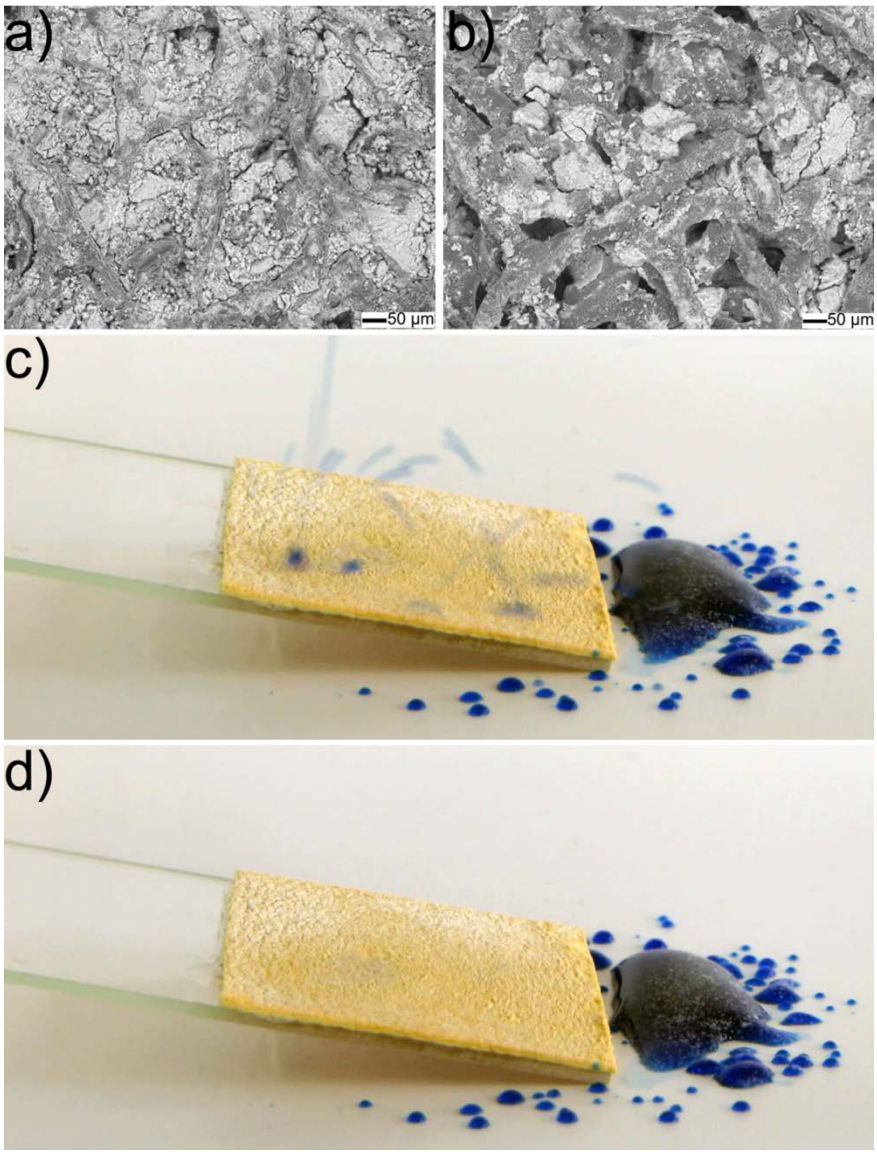

Figure S22. SEM images of an NFCPC before (a) and after (b) the immersion in toluene for 5 days. (c, d) After the immersion, the water extruded from a syringe needle (25 G) dropped on the NFCPC and entirely bounced off the surface, indicating robust water repellency.

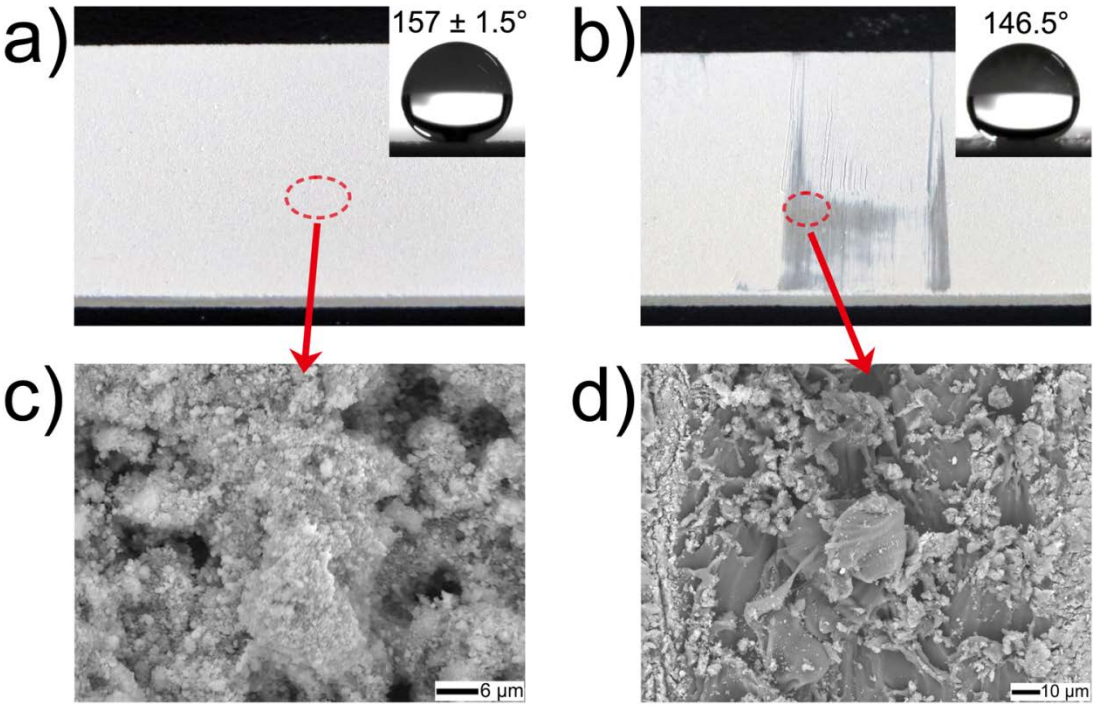

Figure S23. Photographs of a superhydrophobic glass surface including "paint + adhesive" before (a) and after (b) the 10 cm abrasion with grit no. 600 sandpaper under a pressure of 24 kPa. Insets: the corresponding water contact angles. SEM images of the superhydrophobic glass surface before (c) and after (d) the sandpaper abrasion.

The protection of the adhesive for nanoroughness can be immediately broken after the overloaded abrasion, leading to an impaired area with the adhesion of water.